JCTC Journal of Chemical Theory and Computation

Computational Study of the Effects of Mutations A156T, D168V, and D168Q on the Binding of HCV Protease Inhibitors

Zhuyan Guo,*,† Andrew Prongay,† Xiao Tong,‡ Thierry Fischmann,† Stephane Bogen,§ Francisco Velazquez,§ Srikanth Venkatraman,§ F. George Njoroge,§ and Vincent Madison†

Departments of Structural Chemistry, Medicinal Chemistry, and Antiviral Therapy, Schering-Plough Research Institute, 2015 Galloping Hill Road, Kenilworth, New Jersey 07033

Received April 25, 2006

Abstract: The effect of the resistance mutations A156T, D168V, and D168Q in HCV protease on the binding of SCH 6, SCH 503034, VX-950, BILN-2061, and compound 1 was evaluated using the free energy perturbation (FEP) approach. All the inhibitors are highly potent against the wild-type enzyme, but their activity was affected differently by the mutants. A156T reduced the activity of SCH 503034, BILN-2061, and VX950 drastically (200−1000-fold) but that of SCH 6 only moderately (27-fold). SCH 503034, SCH 6, and VX-950 were not affected by either mutation D168V or D168Q, but these mutations conferred a high level of resistance to BILN-2061. Comparison of BILN-2061 with its acyclic analogue compound 1 emphasized the importance of inhibitor flexibility in overcoming drug resistance arising from the D168Q mutation. The results from FEP calculations compared well with experimental binding potencies within an error of <1 kcal/mol. Structural analysis was carried out to relate the resistance profiles to the atomic changes in the mutants.

Introduction

Hepatitis C virus (HCV) is a positive-strand RNA virus of the Flaviviridae family.[1] Its genome is translated into a polyprotein of ∼3000 amino acids in infected cells.[2−4] HCV is a major cause of non-A-non-B hepatitis, which can lead to mortality through either cirrhosis-induced hepatic failure or hepatocellular carcinoma. About 170 million individuals worldwide are chronically infected. Currently, the only therapeutic regimens are subcutaneous interferon-α or PEG-interferon-α alone or in combination with oral ribavirin.[5]

As in the case of human immunodeficiency virus (HIV), most efforts to develop antiviral agents for HCV have focused on the inhibition of the key viral protease, helicase, and polymerase enzymes.[6] The serine protease of HCV comprises the N-terminal domain of the NS3 protein and the NS4A cofactor. It is responsible for proteolytic cleavage at the NS3/NS4A, NS4A/NS4B, NS4B/NS5A, and NS5A/NS5B sites of the nonstructural region of the encoded polyprotein and is essential for viral replication.[7] The NS3/NS4A serine protease has been the most extensively studied HCV target.[8]

As in the case of other viruses, the emergence of drug resistance is a major concern in the development of HCV antiviral therapy. During emergence of escape variants, pre-existing minor viral species resistant to the selected drug will gain a growth advantage over the existing wild-type viral population and rapidly become the dominant genotype. Recently the NS3 protease inhibitors BILN-2061 and VX-950 have been reported to reduce viral loads in proof-of-concept clinical trials.[9−11] SCH 503034 has also advanced to clinical studies.[12]

* Corresponding author phone: (908)740-3796; fax: (908)740-4640; e-mail: zhuyan.guo@spcorp.com.
† Department of Structural Chemistry.
‡ Department of Antiviral Therapy.
§ Department of Medicinal Chemistry.

10.1021/ct600151y CCC: $33.50
Published on Web 09/21/2006

Table 1. Chemical Structure and Experimental Fold Increase in Binding Activities K_i (or K_i* To Indicate Covalent Bond) of HCV Protease Inhibitors upon Mutations A156T, D168V, and D168Q[a]

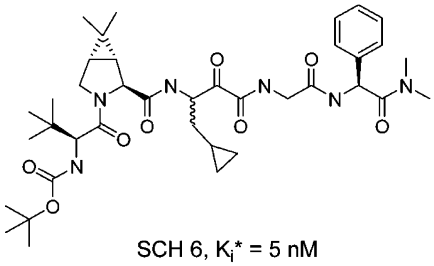

SCH 6, K_i* = 5 nM

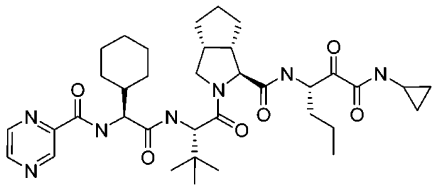

VX-950, K_i* = 50 nM

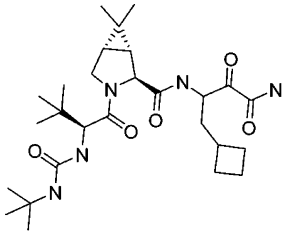

SCH 503034, K_i* = 14 nM

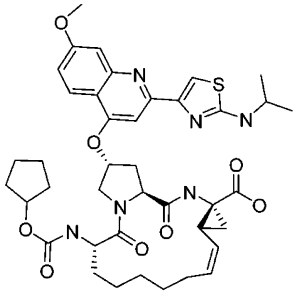

BILN-2061, K_i = 1.2 nM

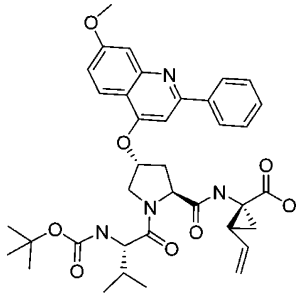

Compound 1, K_i = 14 nM

mutation	SCH 6	SCH 503034	VX-950	BILN-2061	compd1
A156T	27	400	390	1000	
D168V	0.4	1	0.4	260	
D168Q		1	1	70	2

[a] The data were obtained in-house using the assay described.[31]

Protease resistance mutations have been identified by culturing replicon cells in the presence of these and additional inhibitors.[11,13−16] Losses of inhibitor potency have been quantitated,[17,18] and these are summarized in Table 1. The A156T mutation is a major determinant of resistance to BILN-2061, VX-950, and SCH 503034 with increases in K_i or K_i* of 200−1000-fold. In contrast, SCH 6 was still relatively potent against this mutant with only a 27-fold increase in K_i*. Only BILN-2061 was sensitive to mutations of D168 with increases of 260-fold for D168V and 70-fold for D168Q.

In an attempt to elucidate the variations in drug resistance for different HCV protease inhibitors, free energy perturbation (FEP) simulations[19,20] were carried out to study the effects of the two dominant mutations A156T and D168V on the binding of SCH 6, VX-950, BILN-2061, and SCH 503034. In addition, FEP simulations were performed to compare the effects of the D168Q mutation on the binding of BILN-2061 and its acyclic analogue compound 1.[15] This variant occurs in the genotype 3 virus and has been found to have a major impact on the binding of BILN-2061 but does not affect compound 1 or VX-950.[13] Structures from the simulations were analyzed to investigate relationships between the atomic changes of the mutations and the different resistance profiles of these inhibitors.

Materials and Methods

Theory. The FEP method is a general computational approach to determine relative binding free energies.[19−21] It is a thermodynamically rigorous method that is capable of fine structural and energetic distinctions (e.g., $\Delta A < 1$ kcal/mol) in favorable cases. FEP is based on a thermodynamic cycle as depicted in Figure 1 for our mutational studies. Since free energy is a function of state only, the following relation holds for inhibitor *i*

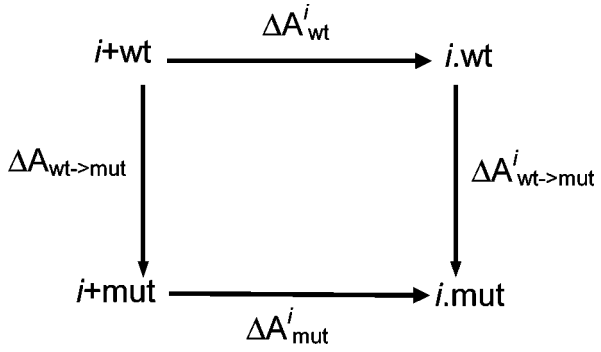

Figure 1. Schematic representation of the thermodynamic cycle. *i*.wt and *i*.mut represent inhibitor *i* bound to the wild-type and mutant enzymes, respectively. *i*+wt and *i*+mut indicate inhibitor *i* and the enzyme in the unbound state.

$$\Delta A^i_{\mathrm{mut}} - \Delta A^i_{\mathrm{wt}} = \Delta A^i_{\mathrm{wt->mut}} - \Delta A_{\mathrm{wt->mut}} \qquad (1)$$

Here ΔA^i_{wt} and $\Delta A^i_{\mathrm{mut}}$ are the free energy of binding of inhibitor *i* to the wild-type and mutant enzymes, respectively, and $\Delta A^i_{\mathrm{wt->mut}}$ and $\Delta A_{\mathrm{wt->mut}}$ are the changes in free energy upon mutation in the presence and absence of inhibitor *i*. When applying eq 1 to both inhibitors *i* and *j*, we obtain the following equation

$$(\Delta A^{j}_{\mathrm{mut}} - \Delta A^{j}_{\mathrm{wt}}) - (\Delta A^{i}_{\mathrm{mut}} - \Delta A^{i}_{\mathrm{wt}}) = \Delta A^{j}_{\mathrm{wt->mut}} - \Delta A^{i}_{\mathrm{wt->mut}} \quad (2)$$

The left-hand side of eq 2, defined to be the relative resistance binding energy $\Delta\Delta A$, is the difference in binding energy between inhibitors *i* and *j* upon mutation and is related to the experimentally observed K_D values as

$$\Delta\Delta A = RT[\ln K_D(j\_\mathrm{mut})/K_D(j\_\mathrm{wt})] - RT\ln[K_D(i\_\mathrm{mut})/K_D(i\_\mathrm{wt})] \quad (3)$$

where $K_D(i\_\mathrm{mut})$ and $K_D(i\_\mathrm{wt})$ are the experimentally observed binding constant for inhibitor *i* with mutant and wild-type enzyme, respectively. In this work, the binding constant is denoted as K_i and K_i*. K_i is the dissociation constant for the inhibitor−enzyme complex exactly analogous to K_D as the dissociation constant for the protein−ligand complex. K_i* is simply an indication that there are two apparent stages to inhibitor binding: one fast and a second slower. K_i* represents the overall dissociation constant for the inhibitor−enzyme complex.

From eq 2, the relative resistance binding energy can also be expressed as

$$\Delta\Delta A = \Delta A^{j}_{\mathrm{wt->mut}} - \Delta A^{i}_{\mathrm{wt->mut}} \quad (4)$$

where $\Delta A^{i}_{\mathrm{wt->mut}}$ and $\Delta A^{j}_{\mathrm{wt->mut}}$ represent the free energy change upon mutation of the wild-type to mutant enzymes in the presence of inhibitors *i* and *j*, respectively. While the quantities on the left side of eq 2 are computationally challenging, $\Delta A^{i}_{\mathrm{wt->mut}}$ and $\Delta A^{j}_{\mathrm{wt->mut}}$ can be obtained through FEP calculations by slowly transforming the wild-type to the mutant enzyme or vice versa.

It is noteworthy that computationally one could mutate either the inhibitor or the protein. However, since the structure of the inhibitors under study differ significantly, we have chosen to mutate the protein side chains; specifically, T156 (mutant) was mutated to Ala (wild-type) and D168 (wild-type) was mutated to either Val or Gln(mutant), in the presence of the inhibitor. In general, mutation from a bulkier to a smaller side chain is preferred computationally, as in the case of T156 to Ala. However, since D168 is situated at the surface of the protein and is solvent exposed, it is less important as to the order of the mutations.

To perform FEP calculations, the wild-type (or mutant) enzyme is converted to the mutant (or wild-type) through a series of theoretical intermediate states by using a coupling parameter λ ($0<\lambda<1$). To overcome sampling problems, simulations with different values of λ have to be performed. The free energy changes for all the λ intervals are added together to obtain the overall free energy change. As a rule of thumb, the free energy change for each λ interval should be less than $2RT$ (R = gas constant, T = temperature) to ensure adequate sampling.[19] Of course, this also depends on the length of the simulation.

Model Building and Simulation Details. The X-ray coordinates for the A156T mutant complexed with SCH 503034 are available in-house (PDB file in preparation). Compared with the inhibitor binding to the wild-type enzyme,[22] the P2 and P3 backbone atoms of the inhibitor have moved away from T156. This is caused by the crowding in that region due to the mutation of A156 to the bulkier Thr residue. This A156T mutant protein structure was used as a starting point for all the A156T calculations. The coordinates of inhibitor SCH 6 were built using SCH 503034 as template. The remaining P1′ and P2′ residues of the inhibitor were modeled based on the crystal structure of this compound binding to the wild-type enzyme (PDB ID 2FM2). The coordinates were then optimized in the A156T mutant protein active site. Similarly, VX-950 was modeled based on SCH 503034, incorporating the binding mode information of an available peptide compound which has the same N-terminal cap (PDB ID 1RGQ). The coordinates of BILN-2061 were obtained from the crystal structure of BILN-2061 complexed with the wild-type enzyme determined in-house. For the D168V and D168Q mutations, the initial coordinates of SCH 503034 were taken from the crystal structure of the inhibitor complexed with the wild-type enzyme.[22] The coordinates of compound 1 were modeled based on the crystal structure of BILN-2061 by removing the P1−P3 macrocycle, modifying the P1 and P3 side chains, and modifying the N-terminal cap. Figure 2 illustrates the binding modes of the inhibitors.

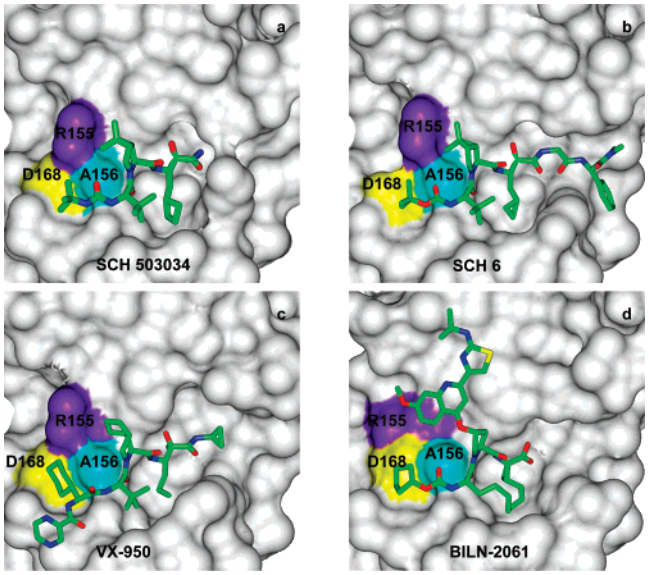

Figure 2. Three-dimensional structures of SCH 503034, SCH 6, VX-960, and BILN-2061 binding to the HCV NS3-NS4A protease. The inhibitors are represented as stick models. Two resistance mutations at A156 (cyan) and D168 (yellow) are colored. R155 which shows a large conformational change upon binding of BILN-2061 is colored purple.

The force field parameters for standard protein residues available in Quanta CHARMM[23] were used. For the nonstandard residues of the inhibitors, atomic charges were assigned consistent with comparable standard residues. Other missing parameters such as bond and torsion angles were assigned by comparison with the parameters involving similar atom types.

The X-ray structures of protease−inhibitor complexes indicate that there is no notable movement in the active site upon inhibitor binding except for a few flexible side chains. Therefore, harmonic restraints were imposed on selected

atoms to prevent unrealistic movement during long dynamics simulations. For residues that are more than 10 Å away from the mutation center, a harmonic restraint with force constant 1.0 kcal/mol-Å^2 (mass weighted) was applied to both the side chain and backbone heavy atoms of the protein. The same harmonic restraint was also applied to the protein backbone atoms within 10 Å of the inhibitor. No restraint was imposed on those side chains that have at least one atom within 10 Å of the inhibitor heavy atoms. A weak harmonic restraint (0.05 kcal/mol-Å^2, mass weighted) was found to be necessary to maintain the observed binding mode for the P2 group of BILN-2061. This mobility of the P2 group may be due to the shallowness of the S2 binding pocket. For consistency, the same restraint was imposed on all the inhibitor heavy atoms.

FEP simulations of the solvated protein−ligand complex were carried out using CHARMM.[24] A total of 11 λ windows for A156T and 38 windows for either D168V or D168Q were used with double-wide sampling. The free energy change within each λ interval was less than 2*RT* (∼1.5 kcal/mol). The protein−inhibitor complex contained 181 residues from NS3 and 14 residues from NS4A plus the inhibitor. The system was centered at the site of mutation. A cap of TIP3P waters was added to fill the space in a 24 Å sphere.[25] The hydrogen atoms were built using CHARMM. During the dynamics simulations, the system temperature was maintained at 300 K. The velocities were reassigned every 200 steps using a Gaussian distribution if the temperature during this period was outside the target 300 K ± 10 K. Bonds involving hydrogen atoms were constrained using the SHAKE algorithm.[26] The time step of the simulation was 1.5 fs. A cutoff of 11 Å was used for nonbonding interactions (electrostatic and van der Waals). A solvent boundary force was used to retain the water molecules.[27] The system was equilibrated for 30 ps followed by 45 ps of data collection for each λ window, and the data were recorded every 10 time steps.

Results and Discussion

FEP simulations on four inhibitors were performed for the A156T mutation. The computational results are reported as relative resistance binding energies $\Delta\Delta A$ using SCH 6 as the reference inhibitor (Table 2). SCH 6 was predicted to be least sensitive to the mutation followed by VX-950, BILN-2061, and SCH 503034 with $\Delta\Delta A$ values ranging from 0.8 to 1.3 kcal/mol. Multiple simulations performed on SCH 6 and VX-950 indicate that the computational statistical error is about 0.5 kcal/mol. For comparison with the computations, experimental fold increase ratios were converted to $\Delta\Delta A$s using eq 3. For SCH 503034, experimental and FEP $\Delta\Delta A$s agree within 0.3 kcal/mol, while the experimental values were underestimated by 0.8 and 0.9 kcal/mol for VX-950 and BILN-2061, respectively. All three values agree within the generally accepted precision estimate for FEP of ∼1 kcal/mol.

For mutations of D168, efforts were focused on BILN-2061 because of its sensitivity to these mutations, while none of the other inhibitors are affected significantly. For D168Q, compound 1 was used as reference to permit a direct comparison of the impact of the macrocycle. For D168V, lacking experimental data for compound 1, SCH 503034 was used as reference due to the availability of its crystal structure. Note that the mutations D168V and D168Q are computationally more challenging because the perturbation of the side chain involves a net change in charge and therefore requires the use of a large number of intermediate states (λ windows) for good convergence. Thus, a total of 38 windows were needed to map the wild-type to the mutant enzyme, compared to 11 windows for the A156T mutation. Nevertheless, computed $\Delta\Delta A$s agree well with experimental values differing by 0.5 and 0.3 kcal/mol for D168V and D168Q, respectively.

Table 2. Relative Resistance Binding Energies (kcal/mol) upon Mutations A156T, D168V, and D168Q[b]

mutation	SCH 6	SCH 503034	VX-950	BILN-2061	compd 1
A156T					
experiment	0.0	1.6	1.6	2.1	
FEP	0.0[a]	1.3	0.8[a]	1.2	
D168V					
experiment		0.0		3.3	
FEP		0.0		2.8	
D168Q					
experiment				2.1	0.0
FEP				2.4	0.0

[a] For SCH 6 and VX-950, multiple simulations were performed, and the average values were used. The original data are SCH 6 = (−0.9, 0.1, 0.3, 0.5), VX-950 = (0.4, 1.2). [b] SCH 6, SCH 503034, and compound 1 are used as references for the A156T, D168V, and D168Q mutations, respectively.

The structural models suggest some factors that contribute to different resistance profiles for the various inhibitors. As in the case of all peptidic, active site inhibitors of HCV protease, there is a network of hydrogen bonds between the backbone atoms of the protease and the inhibitors connecting antiparallel β-strands. Three hydrogen bonds are common to the inhibitors of this study, namely, P1 NH−R155 CO, P3 CO−A157 NH, and P3 NH−A157 CO. Additional hydrogen bonds are formed between the P4 cap C═O of VX-950 and the NH of C159 and P2′ NH of SCH 6 and the carbonyl of T42. Bordering the S2 and S4 pockets, the A156 side chain is in van der Waals contact with the P2 and P3 cap (or P4 for VX-950) groups of the inhibitors. Mutation of A156 to the bulkier Thr causes crowding in that region. As observed in the crystal structure of SCH 503034 complexed with the A156T mutant, the P2−P3 cap backbone atoms shifted away from T156 to avoid crowding (Figure 3). This backbone movement of the inhibitors was also observed in our simulations. This results in weaker hydrogen bonding interactions for both P3 CO−A157 NH and P3 NH−A157 CO. The inhibitor side chains in this region are also crowded. For example, T156 would crowd the P4 cyclohexyl group of VX-950. In turn, the movement of this group would affect inhibitor binding to the S4 and S5 subsites. For BILN-2061 backbone crowding at P2 by T156 would also shift the large P2 side chain, interfering with cation-π interactions between the P2 group and the S2 region of the enzyme to reduce binding affinity. The rigidity of the BILN-2061 macrocycle may also reduce the inhibitor's

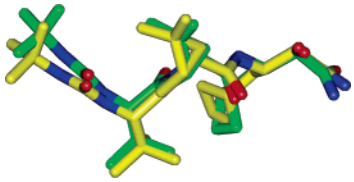

Figure 3. Superimposition of the structures of SCH503034 binding to the HCV NS3-NS4A wild-type and A156T mutant enzymes to illustrate the backbone movement. The carbon atoms are colored green in the wild-type and yellow in the mutant.

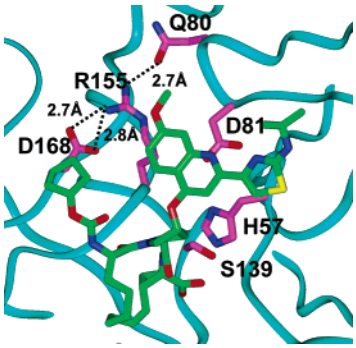

Figure 4. Binding of BILN-2061 to the HCV NS3−NS4A protease. The protein is shown as a ribbon drawing (cyan). The inhibitor is represented as a stick model (green). The side chains of R155, D168, and Q80 are shown (magenta) to illustrate the interactions that stabilize the R155 binding conformation. The catalytic triad S139, H57, and D81 are also displayed.

ability to adapt to changes in the enzyme surface. On the other hand, crowding with the N-terminal cyclopentyl cap could be minimized because of the flexibility of this end of the inhibitor. For SCH 6, decreased binding in the nonprime regions as in SCH 503034 is partially compensated by binding of the C-terminal extension in the P1′ and P2′ sites.

D168 forms salt bridges with the side chains of R123 and R155. As part of the S4 pocket, its methylene group makes van der Waals contacts with the *tert*-butyl group of SCH 503034, cyclopentyl group of BILN-2061, and the P4 cyclohexyl-glycine of VX-950. Based on the structural models, the mutation D168V is not expected to cause steric conflicts. However, as observed in an earlier report,[12] this D168V substitution results in the loss of salt bridge interactions with the R155 side chain which in turn makes extensive contacts with the large P2 group of BILN-2061 (Figure 4). The conformation of R155 in the crystal structure of the BILN-2061−protease complex is no longer energetically favored in the D168V mutant due to the lack of stabilizing interactions. Furthermore, the P2 quinoline group of BILN-2061 would conflict with an alternative conformation of R155 that features a R155−D81 salt bridge as observed in the structures of other inhibitors and the apoprotease.[28] In contrast, SCH 6, SCH 503034, and VX-950 are compatible with this conformation of R155 in the D168V mutation.

Compared to D168V, the D168Q mutation affects the binding of BILN-2061 to a lesser extent, decreasing the binding affinity by only 70 versus 260-fold. This could be explained by the fact that the side-chain carbonyl oxygen of Q168 can still hydrogen bond with the guanidinium group of R155, therefore partially compensating for the loss of the D168-R155 salt bridge interactions to maintain a population of the R155 similar to that in the complex of BILN-2061 and the wild-type enzyme. However, either the difference in this R155 conformation or its lower population causes a 70-fold loss of potency in the D168Q mutant. Apparently, the greater flexibility of the acyclic analogue compound 1 allows it to compensate for these differences. Similar to the D168V mutation, SCH 503034, SCH 6, and VX-950 would not be affected by the mutation D168Q. In another study of genotype specificity, it was observed that the D168Q mutation has no impact on the binding of a set of peptide inhibitors.[29]

In terms of simulations, it is noteworthy that in an earlier work evaluating the effect of P1 substitutions of a product inhibitor on the binding affinity to the HCV protease,[30] no restraint was imposed on the inhibitor, unlike the current work in which a weak constraint was necessary to restrain the inhibitor near its binding conformation. Generally speaking, adding restraints to the inhibitor limits the exploration of alternative binding modes, if any. For the current inhibitors, alternative conformations are unlikely since the backbone conformation is defined by the consensus network of hydrogen bonds. Fixing the backbone leaves little conformational freedom for the side chains except for the P2 groups of BILN-2061 and compound 1.

Conclusions

Employing an all-atom molecular representation of the system with explicit solvent, the FEP method was used to quantify the effect of mutations A156T, D168V, and D168Q in HCV protease on the binding of SCH 6, SCH 503034, VX-950, BILN-2061, and compound 1. All the inhibitors display high potency against wild-type enzyme, but the mutant enzymes are resistant to one or more of the inhibitors. The computed relative resistance energies for the inhibitors agree well with experimental values. Structural analysis identified atomic interactions that allowed each mutant enzyme to be resistant to one or more inhibitors. These results coupled with further FEP calculations and analysis could guide design of inhibitors less susceptible to escape mutants.

Acknowledgment. The authors thank J. Wright-Minogue and E. Xia for generating and assaying the D168Q mutant protease. Z. Guo thanks Drs. J. Duca, J. Voigt, H. Wang, and L. Xiao for helpful discussions and Dr. E. Zaborowski for providing software support. Special thanks to Dr. B. A. Malcolm for careful reading of the manuscript and providing valuable input.

Supporting Information Available: Partial atomic charges of SCH 503034, SCH 6, VX-950, BILN-2061, and compound 1. This material is available free of charge via the Internet at http://pubs.acs.org.

References

(1) Choo, Q. L.; Kuo, G.; Weiner, A. J.; Overby, L. R.; Bradley, D. W.; Houghton, M. Isolation of a cDNA clone derived

from a blood-borne non-A, non-B viral hepatitis genome. *Science* **1989**, *244*, 359−362.

(2) Kato, N.; Hijikata, M.; Ootsuyama, Y.; Nakagawa, M.; Ohkoshi, S.; Sugimura, T.; Shimotohno, K. Molecular cloning of the human hepatitis C virus genome from Japanese patients with non-A, non-B hepatitis. *Proc. Natl. Acad. Sci. U.S.A.* **1990**, *87*, 9524−9528.

(3) Choo, Q. L.; Richman, K. H.; Han, J. H.; Berger, K.; Lee, C.; Dong, C.; Gallegos, C.; Coit, D.; Medina-Selby, R.; Barr, P. J.; Weiner, A. J.; Bradley, D. W.; Kuo, G.; Houghton, M. Genetic organization and diversity of the hepatitis C virus. *Proc. Natl. Acad. Sci. U.S.A.* **1991**, *88*, 2451−2455.

(4) Takamizawa, A.; Mori, C.; Fuke, I.; Manabe, S.; Murakami, S.; Fujita, J.; Onishi, E.; Andoh, T.; Yoshida, I.; Okayama, H. Structure and organization of the hepatitis C virus genome isolated from human carriers. *J. Virol.* **1991**, *65*, 1105−1113.

(5) Houghton, M. Hepatitis C viruses. In *Fields Virology*; 3rd ed.; Fields, B. N., Knipe, D. M., Howley, P. M., Eds.; Lippincott-Raven Publishers: Philadelphia, PA, 1996; pp 1035−1058.

(6) Bartenschlager, R. Candidate targets for hepatitis C virus-specific antiviral therapy. *Intervirology* **1997**, *40*, 378−393.

(7) Kolykhalov, A. A.; Mihalik, K.; Feinstone, S. M.; Rice, C. M. Hepatitis C virus-encoded enzymatic activities and conserved RNA elements in the 3′ nontranslated region are essential for virus replication in vivo. *J. Virol.* **2000**, *74*, 2046−2051.

(8) Bartenschlager, R. The NS3/4A proteinase of the hepatitis C virus: unravelling structure and function of an unusual enzyme and a prime target for antiviral therapy. *J. Viral Hepat.* **1999**, *6*, 165−181.

(9) Lamarre, D.; Anderson, P. C.; Bailey, M.; Beaulieu, P.; Bolger, G.; Bonneau, P.; Bos, M.; Cameron, D. R.; Cartier, M.; Cordingley, M. G.; Faucher, A. M.; Goudreau, N.; Kawai, S. H.; Kukolj, G.; Lagace, L.; LaPlante, S. R.; Narjes, H.; Poupart, M. A.; Rancourt, J.; Sentjens, R. E.; St George, R.; Simoneau, B.; Steinmann, G.; Thibeault, D.; Tsantrizos, Y. S.; Weldon, S. M.; Yong, C. L.; Llinas-Brunet, M. An NS3 protease inhibitor with antiviral effects in humans infected with hepatitis C virus. *Nature* **2003**, *426*, 186−189.

(10) Perni, R. B.; Chandorkar, G.; Chaturvedi, P. R.; Courtney, L. F.; Decker, C. J.; Gates, C. A.; Harbeson, S. L.; Kwong, A. D.; Lin, C.; Lin, K.; Luong, Y. P.; Markland, W.; Rao, B. G.; Tung, R. D.; Thompson, J. A. *Hepatology* **2003**, *38*, Abstr. 972.

(11) Lin, C.; Lin, K.; Luong, Y.; Rao, B. G.; Wei, Y.; Brennan, D. L.; Fulghum, J. R.; Hsiao, H.; Ma, S.; Maxwell, J. P.; Cottrell, K. M.; Perni, R. B.; Gates, C. A.; Kwong, A. D. In *vitro* resistance studies of hepatitis C virus serine protease inhibitors, VX-950 and BILN 2061. *J. Biol. Chem.* **2004**, *279*, 17508−17514.

(12) Malcolm, B. A.; Liu, R.; Lahser, F.; Agrawal, S.; Belanger, B.; Butkiewicz, N.; Chase, R.; Gheyas, F.; Hart, A.; Hesk, D.; Ingravallo, P.; Jiang, C.; Kong, R.; Lu, J.; Pichardo, J.; Prongay, A.; Skelton, A.; Tong, X.; Venkatraman, S.; Xia, E.; Girijavallabhan, V.; Njoroge, F. G. SCH 503034, a Mechanism-based Inhibitor of Hepatitis C Virus NS3 Protease Suppresses Polyprotein Maturation and Enhances the Antiviral Activity of Interferon α. *Antimicrob. Agents Chemother.* **2006**, *50*, 1013−1020.

(13) Tong, X.; Guo, Z.; Wright-Minogue, J.; Xia, E.; Madison, V.; Qiu, P.; Venkatraman, S.; Velazquez, F.; Njoroge, F. G.; Malcolm, B. A. Impact of Naturally Occurring Variants of HCV Protease on the Binding of Different Classes of Protease Inhibitors. *Biochemistry* **2006**, *45*, 1353−1361.

(14) Lin, K.; Kwong, A. D.; Lin, C. Combination of a hepatitis C virus NS3−NS4A protease inhibitor and alpha interferon synergistically inhibits viral RNA replication and facilitates viral RNA clearance in replicon cells. *Antimicrob. Agents Chemother.* **2004**, *48*, 4784−4792.

(15) Trozzi, C.; Bartholomew, L.; Ceccacci, A.; Biasiol, G.; Pacini, L.; Altamura, S.; Narjes, F.; Muraglia, E.; Paonessa, G.; Koch, U.; De Francesco, R.; Steinkuhler, C.; Migliaccio, G. In vitro selection and characterization of hepatitis C virus serine protease variants resistant to an active site peptide inhibitor. *J. Virol.* **2003**, *77*, 3669−3679.

(16) Lin, C.; Gates, C. A.; Rao, B. G.; Brennan, D. L.; Fulghum, J. F.; Luong, Y.; Frantz, J. D.; Lin, K.; Ma, S.; Wei, Y.; Perni, R. B.; Kwong, A. D. In vitro studies of cross-resistance mutations against two hepatitis C virus serine protease inhibitors, VX-950 and BILN 2061. *J. Biol. Chem.* **2005**, *280*, 36784−36791.

(17) Yi, M.; Tong, X.; Skelton, A.; Chase, R.; Chen, T.; Pyles, R.; Bourne, N.; Malcolm, B. A.; Lemon, S. M. Mutations conferring resistance to SCH 6, a novel hepatitis C virus NS3/4A protease inhibitor: Reduced RNA replication fitness and partial rescue by second-site mutations. *J. Biol. Chem.* **2006**, *281*, 8205−8215.

(18) Tong, X.; Chase, R.; Skelton, A.; Chen, T.; Wright-Minogue, J.; Malcolm, B. A. SCH 503034 Resistance Mutations Reduce Fitness of HCV Replicon. *Antiviral Res.* **2006**, in press.

(19) Beveridge, D. L.; DiCapua, F. M. Free energy via molecular simulation: Applications to chemical and biomolecular systems. *Annu. Rev. Biophys. Biophys. Chem.* **1989**, *18*, 431−492.

(20) Kollman, P. Free energy calculations: application to chemical and biochemical phenomena. *Chem. Rev.* **1993**, *93*, 2395−2417.

(21) Udier-Blagoviæ, M.; Tirado-Rives, J.; Jorgensen, W. L. Structural and Energetic Analyses of the Effects of the K103N Mutation of HIV-1 Reverse Transcriptase on Efavirenz Analogues. *J. Med. Chem.* **2004**, *47*, 2389−2392.

(22) Prongay, A. J.; Guo, Z.; Fischmann, T.; Strickland, C.; Myers, J. J.; Yao, N.; Weber, P. C.; Malcolm, B. A.; Beyer, B. M.; Ingram, R.; Pichardo, J.; Hong, Z.; Prosise, W. W.; Ramanathan, L.; Taremi, S. S.; Yarosh-Tomaine, T.; Zhang, R.; Arasappan, A.; Bennett, F.; Bogen, S. L.; Chen, K.; Jao, E.; Liu, Y.; Lovey, R. G.; Saksena, A. K.; Venkatraman, S.; Girijavallabhan, V.; Njoroge, F. G.; Madison, V. Discovery of the HCV NS3/4A Protease Inhibitor SCH503034 II. Key Steps in Structure-Based Optimization. *J. Med. Chem.* **2006**, unpublished results.

(23) Momany, F.; Rone, R. Validation of the general purpose QUANTA 3.2/CHARMM force field. *J. Comput. Chem.* **1992**, *13*, 888−900.

(24) Brooks, B. R.; Bruccoleri, R. E.; Olafson, B. D.; States, D. J.; Swaminathan, S.; Karplus, M. CHARMM: A program for macromolecular energy, minimization, and dynamics calculations. *J. Comput. Chem.* **1983**, *4*, 187−217.

(25) Jorgensen, W. L.; Chandraseklar, J.; Madura, J. D.; Impey, R. W.; Klein, M. L. Comparison of simple potential functions for simulating liquid water. *J. Chem. Phys.* **1983**, *79*, 926−935.

(26) Ryckaert, J. P.; Ciccotti, G.; Berendsen, H. J. C. Numerical integration of the Cartesian equations of motion of a system with constraints: Molecular dynamics of n-alkanes. *J. Comput. Phys.* **1977**, *23*, 327−341.

(27) Brooks, C. L., III.; Karplus, M. Deformable stochastic boundaries in molecular dynamics. *J. Chem. Phys.* **1983**, *79*, 6312−6325.

(28) Di Marco, S.; Rizzi, M.; Volpari, C.; Walsh, M. A.; Narjes, F.; Colarusso, S.; De Francesco, R.; Matassa, V. G.; Sollazzo, M. Inhibition of the hepatitis C virus NS3/4A protease. *J. Biol. Chem.* **2000**, *275*, 7152−7157.

(29) Beyer, B. M.; Zhang, R.; Hong, Z.; Madison, V.; Malcolm, B. A. Effect of naturally occurring active site mutations on hepatitis C virus NS3 protease specificity. *Proteins: Struct., Funct., Genet.* **2001**, *43*, 82−88.

(30) Guo, Z.; Durkin, J.; Fischmann, T.; Ingram, R.; Prongay, A.; Zhang, R.; Madison, V. Application of the λ-dynamics method to evaluate the relative binding free energies of inhibitors to HCV protease. *J. Med. Chem.* **2003**, *46*, 5360−5364.

(31) Zhang, R.; Beyer, B. M.; Durkin, J.; Ingram, R.; Njoroge, F. G.; Windsor, W. T.; Malcolm, B. A. A Continuous Spectrophotometric Assay for the Hepatitis C Virus Serine Protease. *Anal. Biochem.* **1999**, *270*, 268−275.

CT600151Y